Soft Matter

Cite this: *Soft Matter*, 2012, **8**, 2705

www.rsc.org/softmatter

PAPER

Influence of observation temperature on light scattering of poly-*N*-isopropylacrylamide hydrogels†

Saadet Dogu and Wilhelm Oppermann*

Received 7th December 2011, Accepted 15th December 2011
DOI: 10.1039/c2sm07316a

Static and dynamic light scattering methods were applied to characterize the microstructure of gels synthesized by cross-linking copolymerization of *N*-isopropylacrylamide, with particular emphasis on the influence of measurement temperature. The total scattering intensity was divided into two parts: thermal scattering due to Brownian motion and static scattering due to topological or spatial inhomogeneity. Different methods of data evaluation, *i.e.* the non-ergodic and the partial heterodyne approaches, were carefully compared. We obtained consistent results clearly demonstrating that both parts of the scattering rise markedly upon increasing the observation temperature from 10 to 27.5 °C thus approaching the lower critical solution temperature. While the temperature dependence of the thermal scattering component is well understood, we attribute the rise of the static component to the establishment of local swelling equilibrium in a gel whose cross-link density features some inhomogeneity. This means that with rising temperature the more densely cross-linked regions deswell at the expense of the less densely cross-linked ones. As a result, the scattering contrast is enhanced thus leading to a larger static scattering intensity.

Introduction

Polymer gels are cross-linked systems composed of polymer and solvent. Since they have many practical applications such as in contact lenses, super absorbents, *etc.* many research groups concentrate on characterizing them and improving their properties. It is well established that polymer gels generally possess some kind of structure on length scales larger than the mesh size of the network. This is due to an uneven topological or spatial distribution of cross-links and, accordingly, polymer concentration, commonly referred to as spatial gel inhomogeneity, and can be caused by cyclization reactions, microgel formation during preparation, differences between the reactivities of functional groups, and diffusion controlled reactions.[1,2] Although it is of considerable interest and attempts to attain detailed insight have been ongoing for decades, it is still not fully understood.

Light scattering and neutron scattering techniques are most frequently applied to investigate the structure and, in particular, the spatial inhomogeneities in gels. In the light scattering regime (low q-range, $q \ll 0.1$ nm^{-1}), the scattering intensity from gels is generally markedly larger than that from a corresponding polymer solution, while the differences between gel and solution diminish significantly in the higher q-range ($q \gg 0.1$ nm^{-1}) covered by small angle neutron scattering. The excess scattering is related to spatial inhomogeneity, and a number of theoretical approaches or models have been proposed for its interpretation.[3–11] Another manifestation of the inhomogeneity is the appearance of a speckle pattern when a gel is illuminated with coherent light. In dynamic light scattering experiments, it is then observed that different locations within a gel scatter differently.[12–16] Procedures to divide the total scattering intensity into two parts originating from thermal concentration fluctuations and from spatial network heterogeneity were developed in the early 90s.[15,17]

In this paper, we consider both static and dynamic light scattering methods to characterize the microstructure of gels synthesized by cross-linking copolymerization of *N*-isopropylacrylamide (NIPA).

Poly-*N*-isopropylacrylamide (PNIPA) in water forms a temperature sensitive polymer–solvent system with a lower critical solution temperature (LCST) around 34 °C. It is the prime example of a stimuli-responsive polymer, and an extensive literature exists covering studies of, *e.g.*, its phase behavior,[18–20] its potential in creating "intelligent" materials or devices,[21–23] *etc.* Likewise, investigations on PNIPA gels by scattering methods are numerous. Shibayama *et al.* demonstrated that the spatial inhomogeneities increased with rising cross-link concentration and with rising preparation temperature of the gels.[24] They also showed that the ensemble-average light scattering intensity increased when the gels were swollen, while the fluctuating part of the scattering intensity seemed to decrease upon swelling.[25] The same group studied the effect of pressure at gel preparation,[26,27] and they explored the influence of weak ionization of the

Institute of Physical Chemistry, Clausthal University of Technology, Arnold-Sommerfeld-Str. 4, 38678 Clausthal-Zellerfeld, Germany. E-mail: wo@tu-clausthal.de

† Electronic supplementary information (ESI) available. See DOI: 10.1039/c2sm07316a

polymer on the structure factor.[28–30] Wu *et al.* studied the properties of PNIPA hybrid gels formed when a sufficiently concentrated dispersion of microgels was cooled from temperatures above the LCST to below the LCST.[31,32] Their light scattering investigations showed that the static scattering component of the macroscopic gel attained by close-packing of the swollen microgel particles was due to large voids. These could be avoided when the temperature change occurred very slowly.[31]

Surprisingly, papers focusing on a detailed inspection of the dependence of scattering behavior on the observation temperature in the one phase region, below the LCST, are rather scarce. The main emphasis was focused on a study of the critical behavior and the collapse. Already in 1994, Tanaka *et al.* pointed out that the static spatial fluctuations reversibly increased with rising temperature and diverged at the spinodal line.[13] This statement was applied to measurements close to the LCST ($T >$ 25 °C), while data at lower temperatures were somewhat ambiguous. Later, Shibayama *et al.* confirmed the observation that the static and the fluctuating part of light scattering intensity, as well as the cooperative diffusion coefficient, are strongly dependent on the observation temperature.[14] While this was expected for the latter two quantities, the authors concluded that there must be a strong coupling between static and fluctuating components. Koizumi *et al.* deduced from neutron scattering and spin echo data that, as the temperature was raised towards the LCST, the static scattering intensity increased more rapidly than the thermal component.[33] They explained this behavior *via* the excluded volume parameter in the Panyukov Rabin theory, even though the theory was derived for gels made by instantaneous cross-linking of semidilute polymer solutions, which does not apply to the PNIPA gels studied.

The present study aims at a careful inspection of the influence of temperature on the static and thermal scattering components of PNIPA gels in the range 10–27.5 °C, *i.e.* below the LCST. Specifically, for a gel synthesized at 25 °C, light scattering measurements were performed at 25, 20, 15, 10, 12.5, 17.5, and 27.5 °C (in that sequence) in order to verify that the scattering properties are fully reversible with regard to a temperature variation within the range studied. Obviously, the thermal scattering should rise when the LCST is approached from lower temperatures. The dependence of the static scattering on temperature is not so clear and the few literature data diverge to some extent. In order to extract the excess part from dynamic light scattering experiments, we apply the non-ergodic and partial heterodyne approaches,[15–17,34–38] thus separating the contributions of the dynamic or thermal concentration fluctuations and of the (static) inhomogeneities to the total scattering intensity. We also use the much simpler approach based on static scattering for comparison. We will show that both methods agree very well and that the static scattering varies with temperature to the same degree or slightly stronger than the thermal scattering.

Consideration of light scattering and data evaluation

In this paper, we will discuss the information obtained by light scattering methods on the microstructure of hydrogels. Two experimental methods have been applied, which, for simplicity, are referred to as static light scattering (SLS) and dynamic light scattering (DLS). In the current context, the use of these denotations may be somewhat misleading, because the dynamics is not our main concern. We just refer to DLS, when we employ an apparatus that is particularly devised and suited for DLS measurements, but we consider appropriate averages of scattering intensities. Analysis of the dynamics naturally yields the cooperative diffusion coefficient, but it is primarily required to be able to identify different fractions of the total scattering intensities. We will therefore review and compare the two methods with regard to what seems to be relevant for measurements on gels.

Scattering intensities obtained by SLS are usually reported in absolute units as Rayleigh ratios, $R(q)$. Here, $q = (4\pi n/\lambda_0)\sin(\theta/2)$ is the amplitude of the scattering vector with θ being the scattering angle, λ_0 the wavelength of the incident light in a vacuum and n the refractive index of the medium, respectively. For gels, we then write[5–11]

$$R(q) = R_F(q) + R_C(q), \quad (1)$$

where the total scattering intensity, $R(q)$, has been split into two contributions: $R_F(q)$, termed the dynamic or fluctuating part, is due to thermal concentration fluctuations and $R_C(q)$, termed the static part, is due to spatial inhomogeneities possibly resulting from the cross-linking process. The latter is the quantity of interest to characterize the microstructure of the gels.

In a common SLS device, the detector has a wide aperture or slit, collecting the scattered light in a rather large solid angle Ω (typically of the order of 10^{-3}). This results in a correspondingly small coherence area of order λ^2/Ω,[39] which is much smaller than the cross-section of the scattering volume. As a consequence, SLS measurements automatically report the scattering intensity as an ensemble average over the scattering volume. This comes usually pretty close to the macroscopic ensemble. Therefore, all quantities in eqn (1) represent ensemble averages.

In an experimental approach to determine $R_C(q)$ from SLS measurements, one often presumes that the thermal fluctuations in a gel are practically identical with those in a solution of the linear polymer,[6] hence $R_F(q) \approx R_{SOL}(q)$, and $R_C(q) \approx R(q) - R_{SOL}(q)$. $R_{SOL}(q)$ becomes available by separately measuring the scattering intensity of a (semi-dilute or concentrated) solution of the uncross-linked polymer under conditions equivalent to those in the gel. Although this seems to be a plausible assumption, it is not generally valid. Geissler *et al.* showed by a series of carefully devised experiments based on a thorough theoretical treatment that $R_F(q)$ is generally some 30% larger than $R_{SOL}(q)$.[40–42] In many cases, however, the static scattering intensity is so much larger than the thermal scattering that the appreciable error in $R_F(q)$ becomes irrelevant or is plainly accepted. On the other hand, it is frequently difficult or even impossible to prepare a solution of the linear polymer. Either a polymer of exactly the same composition as that in the gel is not available, or the preparation of a homogeneous solution proves impractical because the viscosity is becoming too high.

In DLS, the detection optics is designed to achieve a large coherence factor. Modern instruments employ single-mode or few-mode light guides for this purpose.[43,44] As a consequence, minor changes of the position or orientation of a gel sample produce marked variations of the measured scattering intensity, forming a so-called speckle pattern. While this behavior is typical

of non-ergodic samples such as gels or disordered solids, it does not appear in fluids.

It is common in the literature on DLS to denote the scattering intensity by $I(q)$. We stick to this custom, but we will report these intensities in absolute units to enable direct comparison with data measured by SLS. Hence, $I(q)$ and $R(q)$ are equal quantities, the different letters just refer to distinct measuring methods. Since it is the major purpose of DLS to measure intensities on the scale of μs and to analyze temporal intensity fluctuations, we explicitly indicate time averages by $\langle \ldots \rangle_T$.

As stated above, the time-averaged scattering intensity $\langle I(q) \rangle_T$ measured on a gel sample varies markedly with sample position or orientation. $\langle I(q) \rangle_T$ has two contributions which can be written as[15,17,35]

$$\langle I(q) \rangle_T = \langle I_F(q) \rangle_T + I_C(q) \quad (2)$$

Eqn (2) seems very similar to eqn (1), but there is a significant difference. Whereas eqn (1) applies to the sample as a whole because the intensities are ensemble averages, eqn (2) applies only to one particular speckle, *i.e.* a definite location in the sample observed under a definite scattering vector. $\langle I_F(q) \rangle_T$ is the time average of the fluctuating component arising from dynamic, liquid-like concentration fluctuations. Because this contribution is ergodic, $\langle I_F(q) \rangle_T = R_F(q)$. On the other hand, $I_C(q)$ is independent of time, but depends on position.[45] That is why generally $I_C(q) \neq R_C(q)$ and $\langle I(q) \rangle_T \neq R(q)$. The remainder of this section is therefore concerned with determining the ensemble averages $\langle I(q) \rangle_E$ or $\langle I_C(q) \rangle_E$, respectively.

$\langle I(q) \rangle_E$ can of course be obtained by taking measurements of scattering intensity on a sufficiently large number of positions and subsequent averaging, or by rotating the sample while the measurement is running. But these procedures alone do not allow for a separation of the different contributions. For that purpose, it is necessary to make use of the intensity correlation functions.

Basically, there are two approaches that have been described and discussed extensively in the literature. We therefore just quote the relevant equations used to analyze the experimental data.

According to Pusey and van Megen[17] (non-ergodic method), $\langle I_F(q) \rangle_T$ is related to $\langle I(q) \rangle_T$ *via*

$$\langle I_F(q) \rangle_T = \langle I_F(q) \rangle_E = \langle I(q) \rangle_E [1 - f(q, \infty)] \quad (3)$$

where $f(q,\tau)$ is the normalized intermediate ensemble-averaged scattering function and $f(q,\infty)$ its asymptotic value at $\tau \rightarrow \infty$. $f(q,\tau)$ can in turn be calculated from the time-averaged intensity correlation function measured at a particular position, $g_T^{(2)}$:

$$f(q,\tau) = 1 + \frac{\langle I(q) \rangle_T}{\langle I(q) \rangle_E} \left[\sqrt{\frac{g_T^{(2)}(q,\tau) - 1 - \sigma^2}{\beta}} + 1 - 1 \right] \quad (4)$$

with

$$g_T^{(2)}(q,\tau) = \frac{\langle I(q,0) I(q,\tau) \rangle_T}{\langle I(q,0) \rangle_T^2} \quad (5)$$

and $\sigma^2 = g_T^{(2)}(q,0) - 1$, the initial amplitude of the time-averaged intensity correlation function, and the coherence factor of the instrument, β.

The great attractiveness of this scheme is due to the fact that, in principle, the measurement of just one intensity correlation function at one particular position and the determination of the time-averaged scattering intensity at this position, $\langle I(q) \rangle_T$, are sufficient to identify all desired quantities, provided we have measured $\langle I(q) \rangle_E$ otherwise (*cf.* above). $f(q,\tau)$ values calculated from different $g_T^{(2)}(q,\tau)$ values characterizing different sample positions should be identical for a given system. The accuracy of this method, often termed the *non-ergodic approach* (NE), has also been assessed.[46]

The alternative method, the *partial heterodyne method* (PH),[15] is applicable if intensity correlation functions have been determined on a (large) number of positions. Then, apparent diffusion coefficients D_A can be estimated according to:

$$D_A = -\frac{1}{2q^2} \lim_{\tau \rightarrow 0} \frac{\partial}{\partial t} \ln \left(g_T^{(2)}(q,\tau) - 1 \right) \quad (6)$$

For different sample positions, different values of D_A are obtained, and these come along with different local scattering intensities $\langle I(q) \rangle_T$. A relationship between D_A and the cooperative diffusion coefficient, D, has been derived:

$$D = (2 - \langle I_F(q) \rangle_T / \langle I(q) \rangle_T) D_A \quad (7)$$

Rearrangement of eqn (7) shows that a plot of $\langle I(q) \rangle_T / D_A$ *versus* $\langle I(q) \rangle_T$ should yield a straight line, from the slope and intercept of which the fluctuating component of the scattering intensity, $\langle I_F(q) \rangle_T$, as well as D can be obtained. A sufficiently large number of data points are needed in order to define the straight line with adequate accuracy.

Both approaches described allow separation of the ensemble averaged scattering intensity into its components, $\langle I_F(q) \rangle_E$ and $\langle I_C(q) \rangle_E$. A separate measurement on a solution, as in the case of SLS, is not required.

Experimental section

Synthesis of hydrogels and general characterization

N-Isopropylacrylamide (NIPA, ACROS), *N*,*N*′-methylenebis(acrylamide) (MBA, Sigma), ammonium persulfate (APS, Sigma), and *N*,*N*,*N*′,*N*′-tetramethylethylenediamine (TEMED, Sigma) were used as received. PNIPA gels were prepared by free-radical cross-linking copolymerization of NIPA and MBA in aqueous solutions. The initial monomer concentration C_{NIPA} was fixed at 704.2 mmol L^{-1} while the cross-linker concentration C_{MBA} was varied from 2.8 to 10.0 mmol L^{-1}. A corresponding solution of the linear polymer was prepared under identical conditions without addition of MBA. The polymerization reactions were initiated using 3.5 mmol L^{-1} APS and 16.7 mmol L^{-1} TEMED. First, NIPA, MBA and TEMED were dissolved in distilled water and then the solution was purged with nitrogen gas for 10 min. After addition of the required amount of an APS solution, one part of the mixture was transferred between the plates of the rheometer maintained at the desired preparation temperature, T_{prep} (10, 15, 20, or 25 ± 0.2 °C), and the remaining part was filtered through Teflon membrane filters (pore size: 0.45 μm) directly into NMR tubes serving as light scattering vials. Polymerization took place in these tubes being submerged in a water bath kept at the particular T_{prep}. NMR tubes were

chosen because of their small wall thickness of ~0.6 mm, thus ensuring good heat transfer preventing a temperature rise due to the large negative enthalpy of polymerization.

The LCST was checked by visual inspection of several samples while slowly rising their temperature in a water bath. The solution became turbid at 33.0 °C (sharp transition), while for the gels a more gradual transition was observed with the onset of barely visible turbidity at 29–30 °C followed by a noticeable increase of turbidity at 33.5–34.5 °C. This behavior was confirmed by measuring the transparency in a spectrometer at 500 nm.

In supplemental experiments, weighed hydrogel samples were immersed in a large excess of water for 3 weeks to extract any soluble species. The water was replaced every second day. Eventually, the gels were dried in an oven at 55 °C and weighed again. The gel fraction was determined as the final weight of the dry sample divided by the mass of monomer plus cross-linker in the initial gel sample. We found gel fractions of 90 ± 1%.

Light scattering measurements

SLS and DLS measurements were carried out at observation temperatures, T_{obs}, between 10 °C and 27.5 °C in steps of 2.5 °C. Specifically, for a gel synthesized at $T_{prep} = 25$ °C, light scattering measurements were performed at 25, 20, 15, 10, 12.5, 17.5, and 27.5 °C (in that sequence). Similar experiments were performed on gels synthesized at $T_{prep} = 20$ °C and 15 °C. Both apparatuses were employed with a He–Ne laser operating at $\lambda_0 = 633$ nm and were calibrated against a toluene standard for absolute intensity. SLS was performed on a goniometer SLS-2 (Fica). For measurements on gels, the cuvette was rotated about 60° between each cycle of data sampling to obtain the correct spatial averaging. For DLS, an ALV/CGS-3 compact goniometer (ALV, Langen, Germany) was used equipped with a cuvette rotation/translation unit (CRTU). A fiber optical detection unit based on three-mode detection was used, which includes an appropriate collimator/GRIN-lens fiber and the ALV/STATIC and DYNAMIC enhancer. Ideally, the three-mode detection unit gives an intercept in the time-averaged intensity autocorrelation function (ICF) $g_T^{(2)}(q,0) - 1$ of 0.33; *i.e.*, β should be 0.33. An experimental check with a polystyrene latex suspension gave a coherence factor β of 0.36 ± 0.01, and this value was used for the evaluation of the DLS measurements. To protect the detector, the intensity of the incident light is automatically attenuated at each measurement by an eight-step automatic software-controlled attenuator and measured with a monitor diode. Thus, the intensity of incident light can be different within a series of measurements. When discussing scattering intensities, we therefore use data that were rescaled to a preset value of the monitor diode assuming a linear count rate dependence. Toluene was used as the index matching liquid. The temperature was controlled with an external thermostat. The time averaged ICFs were acquired at 100 different sample positions selected by randomly moving the CRTU before each run. The acquisition time for each run was 30 s. The ensemble-averaged scattering intensity, $\langle I(q)\rangle_E$, was determined by continuously moving the sample vial with the CRTU, and the acquisition time for $\langle I(q)\rangle_E$ was 2 min.

Rheological experiments

The shear moduli of the gels were measured with a parallel-plate rheometer (CVO Rheometer, Bohlin Instruments) equipped with a Peltier device for temperature control. The plates (diameter 40 mm) were set to a distance of 500 μm before the onset of the reactions. During all rheological measurements, a solvent trap was used to minimize solvent evaporation. A frequency of 1 Hz and a deformation amplitude of $\gamma_0 = 0.01$ were selected to ensure that the oscillatory deformation is within the linear regime. The polymerization process was monitored *in situ* by measuring the storage modulus G' and loss modulus G'' as a function of time with the temperature being maintained at the desired T_{prep}. Both moduli reached final constant values after a few hours indicating completion of the polymerization. Then the temperature was changed in steps of 5 °C and the modulus was determined at temperatures different from T_{prep} to obtain data at 15, 20, and 25 °C.

Results and discussion

1. Macroscopic characterization of the PNIPA gels

The hydrogels considered in this paper were all synthesized *via* free radical copolymerization of NIPA and MBA in an aqueous solution. The initial NIPA concentration C_0 was kept constant at 704.2 mmol L^{-1} (80 g L^{-1}) while the cross-linker concentration was varied between 2.81 mmol L^{-1} (0.4% of monomer) and 10.0 mmol L^{-1} (~1.5% of monomer). Gels were prepared at T_{prep} = 10, 15, 20, and 25 °C. In the subsequent discussion, we will focus on the gels made at 25 °C unless otherwise stated. The results obtained for gels made at the other preparation temperatures show essentially similar behavior; typical examples are given in the ESI†.

For a macroscopic characterization, the shear modulus was measured and evaluated according to rubber elasticity theory yielding an estimate of the effective network density, ν_{eff}, according to:[47,48]

$$G' = \nu_{eff}(1 - 2/f) \times R \times T \times \langle r^2\rangle/\langle r^2\rangle_0 \quad (8)$$

Here f is the functionality of the cross-links, hence for tetrafunctional cross-links, $1 - 2/f = 0.5$; R is the gas constant, and T the absolute temperature. $\langle r^2\rangle$ is the mean-square end-to-end distance of network chains and $\langle r^2\rangle_0$ the corresponding quantity for free chains. The calculation according to eqn (8) assumes that G', which is measured at 1 Hz, is identical to the equilibrium modulus within experimental error. This fact was substantiated by the finding that $G''/G' \leq 0.01$ in each case. However, G' showed an unusually strong temperature dependence, decreasing about 12% when the measurement temperature was lowered from 25 °C to 15 °C. Similar dependencies were found for gels made at 15 and 20 °C. The change with temperature was fully reversible. Possibly, this is due to a decrease of $\langle r^2\rangle_0$ when the temperature approaches the LCST from below. Formation of associations represents another possibility that cannot be excluded. (G' rises even stronger above the LCST.) To estimate ν_{eff}, we used G'(25 °C) and assumed $\langle r^2\rangle/\langle r^2\rangle_0 = 1$ under preparation conditions.

Table 1 contains a list of the shear moduli of the gels prepared with different cross-linker concentrations and the quantities

derived thereof. In addition to the effective network density, we have calculated the average molar mass of the network chains, M_C, according to $M_C = C_0/\nu_{eff}$, where C_0 is the mass concentration. The large values obtained for M_C indicate that an effective network chain is likely to consist of branched and cycled structures.

It is useful to compare the effective network density, ν_{eff}, with the hypothetical network density, ν_{th}, of a network where all cross-links are perfectly interconnected by elastically effective network chains. This latter quantity was calculated from the molar concentration of the cross-linker in the system, C_{MBA}, by assuming that all cross-linker molecules have completely reacted as tetrafunctional junction points: $\nu_{th} = 2C_{MBA}$. In fact, the cross-linkers may not have completely reacted and the real network may contain a variety of defects, a wide distribution of chain lengths between junction points, and inhomogeneities of cross-link density and connectivity. The ratio ν_{eff}/ν_{th} (cross-linking efficiency) can serve as a measure for the extent of perfection. It is included in Table 1 as well. The values obtained are almost independent of the cross-linker concentration. They are considerably smaller than 1 indicating a preponderance of network imperfections.

2. Microstructure

An aqueous system containing linear PNIPA has a lower critical solution temperature (LCST) around 34 °C (we found 33.0 °C for our system). Below the LCST, it forms a homogeneous solution. However, concentration fluctuations increase when the temperature gets closer to the miscibility gap. Stated otherwise, water is a good solvent for PNIPA at low temperature, but the solvent quality drops significantly with rising temperature. This thermodynamic behavior gives rise to an increase of scattering intensities when the temperature approaches the LCST from below. (The refractive index increment, dn/dc, measured for dilute PNIPA solutions does not change perceptibly with temperature; we found 0.181 mL g^{-1} at 15 °C and 0.182 mL g^{-1} at 25 °C. So the intensities are a good measure for concentration fluctuations.) When PNIPA is cross-linked to form a gel, the visually determined LCST rises slightly and does not appear as sharp as in solution (*cf.* Experimental section). In such gels, the thermodynamic fluctuations are superimposed by static concentration fluctuations that are independent of time, but depend on location. We are particularly interested in the influence of temperature on these static fluctuations.

We will therefore discuss the information obtained by light scattering on the microstructure of the hydrogels and the influence of temperature thereon. The length scale probed by light scattering is of the order of $1/q$, corresponding to 40–90 nm when the scattering angle is in the range 50°–140°. This length scale should be compared with the mean distance between cross-linkages, which is around 5–10 nm based on C_{MBA}. Hence we are looking at structural characteristics appreciably larger than the mesh size of the network.

Table 1 Results of rheological measurements obtained on gels made with different cross-linker concentrations. Monomer concentration C_{NIPA} = 704.2 mM corresponding to 7.15 vol%

C_{MBA}/ mmol L^{-1}	G'(25 °C)/ kPa	ν_{eff}/ mol m^{-3}	M_C/g mol^{-1}	ν_{eff}/ν_{th}
2.81	0.93	0.75	100 000	0.132
4.69	1.80	1.44	55 000	0.154
7.04	2.37	1.91	42 000	0.135
8.80	2.94	2.36	34 000	0.134
10.0	3.25	2.60	31 000	0.131

2.1 SLS. As mentioned further above, SLS measurements automatically report the scattering intensity as an ensemble average over the scattering volume, being close to a macroscopic ensemble. This was verified by repetition of the measurements after turning or shifting the sample and checking for reproducibility. Usually an average over 5 different positions was taken.

To investigate the influence of observation temperature on the microstructure of PNIPA hydrogels, static light scattering experiments were carried out in the range 10 °C ≤ T_{obs} ≤ 27.5 °C on these gels as well as on the corresponding solution. The scattered light intensities, $R(q)$, were recorded at scattering angles from 50° to 140°, which corresponds to a scattering vector range of $q = 1.1 \times 10^5$ to 2.5×10^5 cm^{-1}.

Fig. 1 shows the total scattering intensity $R(q) = R_C(q) + R_{SOL}(q)$ *vs.* the square of the scattering vector q^2 for the hydrogels prepared at 25 °C with various amounts of MBA at different observation temperatures. Increasing the MBA concentration and observation temperature increases $R(q)$ of the hydrogels. The change with temperature is fully reversible. It should be mentioned that $R_{SOL}(q)$ rises from 1.02×10^{-4} cm^{-1} at 15 °C to 1.82×10^{-4} cm^{-1} at 25 °C. These results obviously show that the static portion of the scattered light from the PNIPA hydrogels is strongly temperature dependent. The angular dependence is too small to be exploited.

2.2 DLS. Fig. 2 shows the results of DLS measurements made at $\theta = 90°$ on several gels having different cross-linker contents (b–d), and on a solution of the linear polymer (a). For each sample, 100 measurements were conducted at different sample positions. The observation temperature was 25 °C, identical to the preparation temperature. Fig. 2 clearly demonstrates that the gels exhibit the typical speckle pattern, becoming more pronounced when the cross-linker content was raised, while the scattering intensity observed on the solution is independent of position. This behavior is well known and has been reported repeatedly.

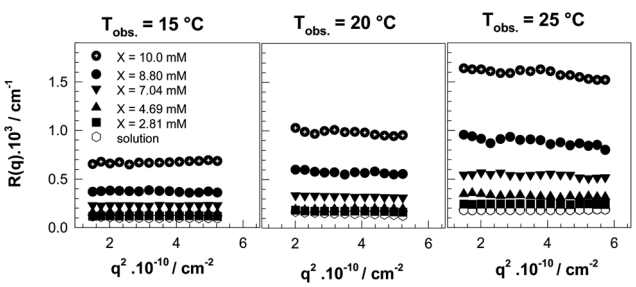

Fig. 1 Total scattering intensity $R(q)$ plotted *versus* q^2 for PNIPA hydrogels at different measurement temperatures, T_{obs}, and MBA concentrations, X, as indicated. T_{prep} = 25 °C.

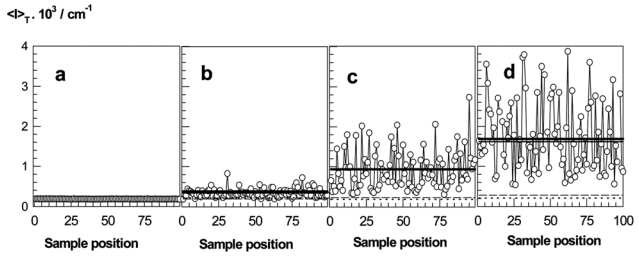

Fig. 2 Variation of time averaged scattering intensity $\langle I\rangle_T$ with sample position for PNIPA hydrogels with (a) 0, (b) 4.69, (c) 8.80, and (d) 10.0 mM MBA concentration. The solid lines represent the ensemble-averaged scattered intensity, $\langle I\rangle_E$. The fluctuating components of the scattering intensity, $\langle I_F\rangle_T$, are represented by the dashed and dotted lines. $T_{obs} = T_{prep} = 25\ ^\circ C$; $\theta = 90^\circ$.

The solid horizontal lines represent the ensemble average of scattering intensity, $\langle I\rangle_E$, obtained, on the one hand, by calculating the mean value of the data obtained at 100 positions, and, on the other hand, the value measured while the cuvette was steadily rotated. There is a slight difference between the two values reflecting experimental uncertainty. The dashed line indicates the fluctuating component of the scattered intensity, $\langle I_F\rangle_T$, estimated by the partial heterodyne method (based on 100 positions, eqn (7)), while the dotted line gives the result for $\langle I_F\rangle_T$ when the non-ergodic method was applied on just 15 positions (eqn (3)), with subsequent averaging. The essential features deduced from Fig. 2 are as follows: there is no appreciable discrepancy between the two methods of data evaluation (we will elaborate on this point further below). While $\langle I\rangle_E$ increases significantly with rising cross-link density, the fluctuating component, $\langle I_F\rangle_T$, remains practically constant and is identical to the scattering intensity of a solution 1.8×10^{-4} cm^{-1}.

To analyze the influence of observation temperature on the scattering behavior, we focus on the sample having 8.8 mmol L^{-1} MBA, shown in Fig. 2c. Fig. 3 shows the corresponding data measured at 10, 15, 20, and 25 °C at $\theta = 90^\circ$. It is obvious that the spatial fluctuations of $\langle I\rangle_T$ grow significantly with rising temperature, and so do the ensemble averages. The change with temperature is fully reversible. Closer inspection shows that the fluctuating component, $\langle I_F\rangle_T$, is also rising with temperature. This is easier seen in a compilation of the data given in Table 2. Columns 2 and 3 represent $\langle I_F\rangle_T$ determined by the partial heterodyne method and the non-ergodic method, respectively. Columns 4 and 5 show, for comparison, the scattering intensity of a PNIPA solution measured in the two apparatus. All 4 values agree to within ±20% at each temperature, while there is a distinct increase with rising temperature. This increase is expected, of course, because the thermal fluctuations become stronger when the LCST is approached.

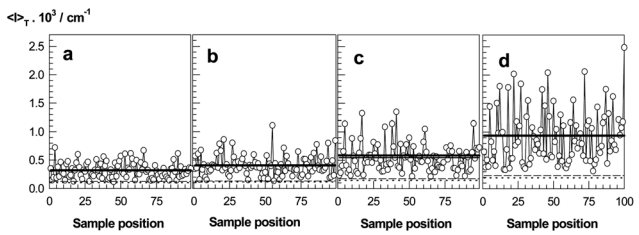

Fig. 3 Variations of time-averaged scattering intensity, $\langle I\rangle_T$, with sample position at 4 different observation temperatures, (a) 10, (b) 15, (c) 20, and (d) 25 °C, for a gel prepared at 25 °C with 8.8 mM MBA. The solid lines represent the ensemble-averaged scattered intensity, $\langle I\rangle_E$. The fluctuating components of the scattering intensity, $\langle I_F\rangle_T$, are represented by the dashed and dotted lines. $\theta = 90^\circ$.

The last three columns in Table 2 show the constant component of scattering intensity, I_C, obtained *via* the partial heterodyne method and the non-ergodic method, respectively, as well as R_C, obtained by SLS (eqn (1)). Again, the data agree satisfactorily at each temperature. However, there is a marked increase with rising temperature, seemingly even stronger than that of $\langle I_F\rangle_T$. This observation requires further discussion.

If one erroneously assumed that the static scattering was due to some permanently fixed, solid-like heterogeneity, there would be no influence of temperature on I_C. Obviously, this is not correct. In fact, the increase of $I_C(q)$ with rising temperature for PNIPA gels below the LCST was already reported by Tanaka *et al.*[13] and Shibayama *et al.*,[14,35] but without giving an in-depth explanation. They showed that above the LCST (36–50 °C) for weakly charged PNIPA gels, I_C rises markedly with increasing observation temperature due to the progressive formation of a two-phase structure, while $\langle I_F\rangle_T$ remains essentially constant.[29]

Considering the scattering behavior in the homogeneous region below the LCST, we proceed from the notion that a given polymer network generally has an inhomogeneous distribution of cross-links. Hence, the local cross-link density (in an area defined by the static correlation length) is fixed through synthesis. This local cross-link density controls the local polymer concentration depending on thermodynamic conditions. It is predominantly the polymer density correlation function that determines the scattering properties of the gel, not the (fixed!) cross-link density correlation function (unless the refractive index increment of the cross-linking moieties is by far greater than that of the polymer). The temperature dependence of the static scattering intensity $I_C(q)$ therefore arises from the thermodynamics of variable local swelling.

The swelling pressure of a gel is given by the osmotic pressure of a semi-dilute solution of the uncross-linked polymer plus the negative pressure due to chain elasticity.[49] The osmotic pressure, as a crude approximation, changes in proportion with excluded volume, or $(1 - 2\chi)$, where χ is the Flory interaction parameter. For PNIPA, χ varies strongly with temperature and approaches 0.5 near the LCST. On the other hand, the pressure due to chain elasticity is nearly independent of solvent quality, but proportional to cross-link density. Now consider regions of high cross-link density in equilibrium with regions of lower cross-link density. At a given temperature, say 20 °C, this equilibrium results in distinct variations of local polymer concentration. As the temperature is raised, the osmotic part of the swelling pressure becomes smaller while the elastic part becomes more dominant. This means that the more densely cross-linked regions deswell at the expense of the less densely cross-linked ones. (The overall volume is kept constant, of course; the gel is not in macroscopic equilibrium with pure solvent.) As a result, the characteristic length scales of the structure do not change, but the scattering contrast is enhanced, resulting in larger static scattering intensity.

Table 2 Intensity values (in 10^{-4} cm^{-1}) of the fluctuating (I_F) and frozen (I_C) part in dynamic and static light scattering at different observation temperatures. $\theta = 90°$, $C_{MBA} = 8.80$ mM, $T_{prep} = 25$ °C

T_{obs}	I_F (PH)	I_F (NE)	$I_{F,SOL}$ (DLS)	$R_{F,SOL}$ (SLS)	I_C (PH)	I_C (NE)	R_C (SLS)
10 °C	1.23	1.03	1.04	0.76	1.95	2.17	1.92
15 °C	1.31	1.14	1.27	1.02	2.82	2.93	2.70
20 °C	1.74	1.46	1.71	1.50	3.73	4.36	4.24
25 °C	2.37	1.92	1.87	1.82	6.99	8.65	7.17

By this argument, the temperature dependence of $I_C(q)$ is traced back to the same origin as that of $\langle I_F(q)\rangle_T$, namely solvent quality. This does not necessarily mean, however, that the form of the dependence is similar. Thermal fluctuations, giving rise to $\langle I_F(q)\rangle_T$, are governed by the course of the spinodal, while the static concentration contrast, giving rise to $I_C(q)$, results from local swelling equilibrium.

In order to compare the temperature dependencies of the two components, it is worthwhile to look at the normalized intermediate scattering functions calculated from the measured $g_T^{(2)}(q,\tau)$ by eqn (4). Fig. 4 shows the averaged $f(q,\tau)$ functions for $q = 1.9 \times 10^5$ cm^{-1} corresponding to a scattering angle of 90°. At long times they reach asymptotic plateau values that increase slightly with rising measuring temperature and that are indicative of the frozen-in inhomogeneity. According to the theory derived by Pusey and van Megen, the $f(q,\tau)$ curves measured at one temperature on a given gel should be identical irrespective of the sample position. Actually, there is quite some scatter in these plateau values. Table 3 therefore shows a list of the average values together with their standard deviations derived from measurements at 15 positions. They were obtained by fitting of the data to the expression

$$f(q,t) = f(q,\infty) + A \exp\left(-\frac{t}{\tau}\right) \quad (9)$$

using a nonlinear least-squares fitting procedure.

$f(q,\infty)$, *i.e.* the (ensemble averaged) fraction of scattered light which is due to static inhomogeneities, increases moderately from around 70% to around 80% when the measuring temperature is raised from 10 °C to 25 °C. This rise is clearly beyond experimental uncertainty and proves that the static scattering component is affected by temperature to a greater extent than the fluctuating component.

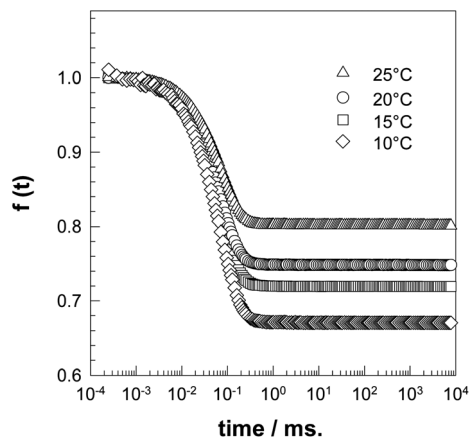

Fig. 4 Normalized intermediate ensemble-averaged scattering functions, $f(t)$, calculated from $g_T^2(\tau)$ values according to eqn (4) for different observation temperatures, $T_{prep} = 25$ °C.

The correlation time, τ, is around 70 μs corresponding to cooperative diffusion coefficients, D, between 35 and 43 μm^2 s^{-1}. D rises moderately with increasing cross-link density, while the influence of temperature is amazingly small (less than 5% change when the observation temperature was increased from 10 to 25 °C, *i.e.* within the experimental error). Since the viscosity of water drops by 30% in that range, there is likely an opposing effect based on some structural rearrangement. The correlation lengths in the range 5–7 nm compare well with the mean distance between cross-links.

Fig. 5 shows a side-by-side comparison of the temperature dependences of scattering intensity measured by SLS and DLS for a range of cross-link densities for gels prepared at 25 °C. (Gels prepared at 20 °C and 15 °C give similar results as shown in Fig. S1 and S2 in the ESI†.) Note that $\langle I_F\rangle_T$ corresponds to R_F and $\langle I\rangle_E$ corresponds to $R(q)$. The two graphs are closely identical. This is of course taken for granted as far as the ensemble-averaged total scattering intensities are concerned. In this case, the two methods just differ in the fact that the SLS apparatus yields the ensemble average directly, while with the DLS apparatus, the averaging must be performed deliberately either by rotating the cuvette during the measurement or by taking the average over a sufficiently large number of measurements taken at different sample positions. The procedures applied to obtain the fluctuating components, however, are fundamentally different. In SLS, the polymerization was carried out without a cross-linker, and the scattering intensity of the resulting solution is *assumed* to represent the fluctuating component of correspondingly synthesized gels. In DLS, the intensity correlation functions obtained on the gels were used to extract the fluctuating part. This could be done for each degree of cross-linking. Fig. 5 shows that the $\langle I_F\rangle_T$ data form one single line (open symbols in Fig. 5a), and that this line is pretty much the same as that of the solution (open symbols in Fig. 5b). These observations strongly support the notion that the two experimental approaches are equivalent. Fig. 5 further demonstrates that the discussion about the slightly different temperature

Table 3 List of the average values of $f(q,\infty)$ together with their standard deviations derived from measurements at 15 positions

T_{obs}	$f(q,\infty)$
10 °C	0.68 ± 0.057
15 °C	0.71 ± 0.047
20 °C	0.74 ± 0.035
25 °C	0.80 ± 0.036

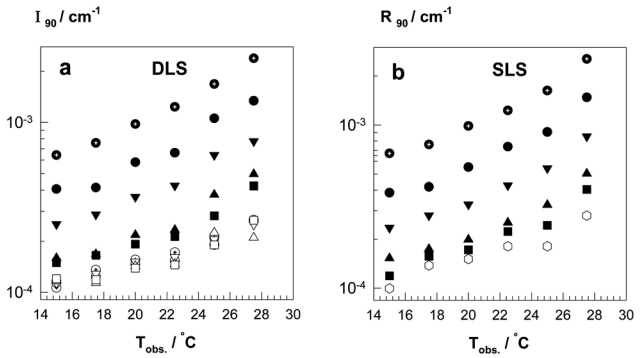

Fig. 5 Comparison of the scattering intensities measured at 90° by DLS (I_{90}) and SLS (R_{90}) as a function of observation temperature for gels prepared at 25 °C. MBA concentrations are: (○) 10.0, (●) 8.8, (▼) 7.04, (▲) 4.69, and (■) 2.81 mM. Open symbols represent the fluctuating components for DLS or the solution scattering for SLS.

dependences of $\langle I_F \rangle_T$ and I_C (or R_F and R_C) is a general phenomenon with PNIPA networks, irrespective of the degree of cross-linking.

It would be interesting to exploit the q-dependence of the static scattering component in order to obtain some information on the length scale of static inhomogeneities. As recognized from Fig. 1, the variation of scattering intensity in the experimentally accessible q-range is too small to be quantified with some confidence. The slope of the intensity *vs.* q^2-plot seems negative (as expected) in some instances, but positive slopes and slopes close to zero are also found. Similar behavior was found by DLS measurements (not shown). This means that the static correlation length does not exceed 10–15 nm, and light scattering experiments are not suited to obtain information at the smaller scale.

Conclusions

Static and dynamic light scattering measurements were performed on PNIPA hydrogels in order to carefully compare different methods of dividing the total scattering intensity into two parts: thermal scattering due to Brownian motion of the network chains and static scattering due to topological or spatial inhomogeneity. All methods investigated yield consistent results and, in the first place, confirm the well-known fact that the static component rises strongly with increasing the cross-link density. The major emphasis of the present work was on a detailed inspection of the dependence on the observation temperature of the thermal and static scattering components of a given gel. Earlier publications[13,14,35] showed that both parts seem to increase when the temperature was raised, but this became evident only in a rather narrow temperature window, from 30–33 °C, close to the LCST. Our present results clearly show that both components also increase perceptibly in the range 10 °C $\leq T_{obs} \leq$ 25 °C, much further away from the LCST of PNIPA in water. The increase of the thermal scattering is expected, of course, because thermal fluctuations become stronger when the LCST is approached. However, the static component of scattering intensity is affected by temperature to an even greater extent. We interpret this behavior by assuming local swelling equilibrium in a gel whose cross-link density features some inhomogeneity. Equilibrium swelling is controlled by two competing factors, osmotic pressure and chain elasticity. The osmotic pressure of a semi-dilute polymer solution given by the Flory–Huggins equation scales, to a first approximation, with excluded volume, or $(1 - 2\chi)$, where χ is the Flory interaction parameter. For PNIPA, χ rises with temperature and approaches 0.5 near the LCST. Hence, the osmotic pressure decreases with rising temperature, while the chain elasticity remains essentially constant. This means that upon raising the temperature, more densely cross-linked regions deswell at the expense of the less densely cross-linked ones. Accordingly, the scattering contrast is enhanced thus leading to a larger static scattering intensity, as first pointed out by Tanaka *et al.*[13]

By following this argument we suppose that both parts of the scattering intensity are governed by thermodynamic quantities, namely quality of the solvent. However, different dependencies apply thus leading to the fact that the static scattering seems to be slightly more sensitive to temperature than the thermal scattering intensity. Our interpretation based on local swelling equilibrium is in accord with the view that polymer gels possess restricted ergodicity.[10] They have an inhomogeneous distribution of cross-links, but their density-inhomogeneity is not fixed. Rather it is dependent on the establishment of local swelling equilibrium controlled by a distinct network topology.

Acknowledgements

We gratefully acknowledge financial support received from the Deutsche Forschungsgemeinschaft (DFG).

References

1 W. Funke, O. Okay and B. Joos-Muller, *Adv. Polym. Sci.*, 1998, **136**, 139–234.
2 O. Okay, *Prog. Polym. Sci.*, 2000, **25**, 711–779.
3 J. Bastide and S. J. Candau, in *Physical Properties of Polymeric Gels*, ed. J. P. Cohen Addad, Wiley, London, 1996, p. 143.
4 P. Debye and A. M. Bueche, *J. Appl. Phys.*, 1949, **20**, 518–525.
5 F. Bueche, *J. Colloid Interface Sci.*, 1970, **33**, 61–66.
6 V. K. Soni and R. S. Stein, *Macromolecules*, 1990, **23**, 5257–5265.
7 J. Bastide and L. Leibler, *Macromolecules*, 1988, **21**, 2647–2649.
8 S. Panyukov and Y. Rabin, *Phys. Rep.*, 1996, **269**, 1–131.
9 F. Horkay, A. M. Hecht and E. Geissler, *J. Chem. Phys.*, 1989, **91**, 2706–2711.
10 S. Panyukov and Y. Rabin, *Macromolecules*, 1996, **29**, 7960–7975.
11 Y. Rabin and S. Panyukov, *Macromolecules*, 1997, **30**, 301–312.
12 F. Ikkai and M. Shibayama, *Phys. Rev. Lett.*, 1999, **82**, 4946–4949.
13 E. S. Matsuo, M. Orkisz, S.-T. Sun, Y. Li and T. Tanaka, *Macromolecules*, 1994, **27**, 6791–6796.
14 M. Shibayama, S.-I. Takata and T. Norisuye, *Phys. A*, 1998, **249**, 245–252.
15 J. G. H. Joosten, J. L. McCarthy and P. N. Pusey, *Macromolecules*, 1991, **24**, 6690–6699.
16 A. Moussaid, S. J. Candau and J. G. H. Joosten, *Macromolecules*, 1994, **27**, 2102–2110.
17 P. N. Pusey and W. van Megen, *Phys. A*, 1989, **157**, 705–741.
18 C. Boutris, E. G. Chatzi and C. P. Kiparissides, *Polymer*, 1997, **38**, 2567–2570.
19 Y. Okada and F. Tanaka, *Macromolecules*, 2005, **38**, 4465–4471.
20 T. Kawaguchi, K. Kobayashi, M. Osa and T. Yoshizaki, *J. Phys. Chem. B*, 2009, **113**, 5440–5447.
21 K.-F. Arndt, T. Schmidt, A. Richter and D. Kuckling, *Macromol. Symp.*, 2004, **207**, 257–268.
22 A. Richter, S. Howitz, D. Kuckling and K.-F. Arndt, *Sens. Actuators, B*, 2004, **99**, 451–458.
23 M. Ballauf and Y. Lu, *Polymer*, 2007, **48**, 1815–1823.
24 S. Takata, T. Norisuye and M. Shibayama, *Macromolecules*, 2002, **35**, 4779–4784.

25 M. Shibayama, Y. Shirotani and Y. Shiwa, *J. Chem. Phys.*, 2000, **112**, 442–449.
26 M. Shibayama, *Polym. J.*, 2010, **43**, 18–34.
27 M. Shibayama, S. Takata and C. Nakamoto, *Macromol. Symp.*, 2004, **207**, 31–36.
28 M. Shibayama, K. Isono, S. Okabe, T. Karino and M. Nagao, *Macromolecules*, 2004, **37**, 2909–2918.
29 M. Shibayama, K. Kawakubo and T. Norisuye, *Macromolecules*, 1998, **31**, 1608–1614.
30 F. Ikkai and M. Shibayama, *J. Polym. Sci., Part B: Polym. Phys.*, 2005, **43**, 617–628.
31 Y. Zhao, G. Zhang and C. Wu, *Macromolecules*, 2001, **34**, 7804–7808.
32 Y. Zhao, Y. Yang and C. Wu, *Macromolecules*, 2003, **36**, 855–859.
33 S. Koizumi, M. Monkenbusch, D. Richter, D. Schwahn and B. Farago, *J. Chem. Phys.*, 2004, **121**, 12721–12731.
34 J. G. H. Joosten, E. T. F. Gelade and P. N. Pusey, *Phys. Rev. A: At., Mol., Opt. Phys.*, 1990, **42**, 2161–2173.
35 M. Shibayama, *Macromol. Chem. Phys.*, 1998, **199**, 1–30.
36 L. Fang and W. Brown, *Macromolecules*, 1992, **25**, 6897–6903.
37 T. Tanaka, L. O. Hocker and G. B. Benedek, *J. Chem. Phys.*, 1973, **59**, 5151–5159.
38 A. B. Rodd, D. E. Dunstan, D. V. Boger, J. Schmidt and W. Burchard, *Macromolecules*, 2001, **34**, 3339–3352.
39 B. J. Berne and R. Pecora, *Dynamic Light Scattering*, Dover Publ., Mineola, NY, 2000, pp. 44–46.
40 A.-M. Hecht, F. Horkay, P. Schleger and E. Geissler, *Macromolecules*, 2002, **35**, 8552–8555.
41 E. Geissler, in *Dynamic Light Scattering*, ed. W. Brown, Oxford University Press, 1993, pp. 471–511.
42 E. Geissler, F. Horkay and A.-M. Hecht, *Phys. Rev. Lett.*, 1993, **71**, 645–648.
43 J. Rička, *Appl. Opt.*, 1993, **32**, 2860–2875.
44 T. Gisler, H. Rüger, S. U. Egelhaaf, J. Tschumi, P. Schurtenberger and J. Rička, *Appl. Opt.*, 1995, **34**, 3546–3553.
45 Macromolecules 2004, **37**, 2944–2953, Norisuye *et al.* reported that $\langle I_F(q)\rangle_T$ is also dependent on the position. However, this variation is extremely small compared to that of $I_C(q)$ and will not be considered here.
46 K. Schätzel, *Appl. Opt.*, 1993, **32**, 3880–3885.
47 P. J. Flory, *Principles of Polymer Chemistry*, Cornell University Press, Ithaca, NY, 1953.
48 L. R. G. Treloar, *The Physics of Rubber Elasticity*, 3rd edn, Clarendon Press, Oxford, UK, 1975.
49 M. Rubinstein and R. H. Colby, *Polymer Physics*, Oxford University Press, Oxford, 2003.